11-25-2019

High-order rogue waves of a long-wave–short-wave model of Newell type

Jungchao Chen
Lishui University

Liangyuan Chen
Lishui University

Bao-Feng Feng
The University of Texas Rio Grande Valley, baofeng.feng@utrgv.edu

Ken-ichi Maruno
Waseda University

High-order rogue waves of a long-wave–short-wave model of Newell type

Junchao Chen,[1,*] Liangyuan Chen,[2] Bao-Feng Feng,[3] and Ken-ichi Maruno[4]

[1]*Department of Mathematics, Lishui University, Lishui, 323000, People's Republic of China*

[2]*Department of Photoelectric Engineering, Lishui University, Lishui 323000, People's Republic of China*

[3]*School of Mathematical and Statistical Sciences, The University of Texas Rio Grande Valley, Edinburg, Texas 78541, USA*

[4]*Department of Applied Mathematics, School of Fundamental Science and Engineering, Waseda University, 3-4-1 Okubo, Shinjuku-ku, Tokyo 169-8555, Japan*

(Received 28 January 2019; revised manuscript received 8 October 2019; published 25 November 2019)

The long-wave–short-wave (LWSW) model of Newell type is an integrable model describing the interaction between the gravity wave (long wave) and the capillary wave (short wave) for the surface wave of deep water under certain resonance conditions. In the present paper, we are concerned with rogue-wave solutions to the LWSW model of Newell type. By combining the Hirota's bilinear method and the KP hierarchy reduction, we construct its general rational solution expressed by the determinant. It is found that the fundamental rogue wave for the short wave can be classified into three different patterns: bright, intermediate, and dark states, whereas the one for the long wave is always a bright state. The higher-order rogue wave corresponds to the superposition of fundamental ones. The modulation instability analysis shows that the condition of the baseband modulation instability where an unstable continuous-wave background corresponds to perturbations with infinitesimally small frequencies, coincides with the condition for the existence of rogue-wave solutions.

DOI: 10.1103/PhysRevE.100.052216

I. INTRODUCTION

Rogue waves (RWs) or freak waves are a rare phenomenon where large amplitudes appear from the background with instability and unpredictability. Such extreme waves can be observed in various different contexts such as oceanography [1], hydrodynamic [2,3], Bose-Einstein condensate [4], plasma [5], and nonlinear optics [2,6,7]. Mathematically, a Peregrine soliton (namely, the first-order rational soliton characterized by a second-order polynomial of temporal and spatial variables) of nonlinear Schrödinger (NLS) equation serves as a prototype of RW, in which its structure is localized in temporal-spatial distribution plane and its maximum amplitude attains three times the background [8–10]. Since the higher-order RW was excited experimentally in wave tanks [11,12], a hierarchy of higher-order analytic RW solutions which indicate the superposition of elementary RW have been found in integrable NLS equation by using different techniques [13–18]. In contrast to the scalar system, recent studies have shown that multicomponent coupled systems may allow several novel patterns of RW such as dark and four-petaled types [19–33]. Indeed, in order to consider different spectral peaks, modes, and polarization states, various physical phenomena usually need to be described by the nonlinear models with two or more components. These multicomponent systems are of physical importance in different branches of science, e.g., hydrodynamics, nonlinear optics, and plasma physics. Regarding the RWs in multicomponent systems, theoretical investigations have been developed in many integrable systems such as the vector NLS equations [19–25], the three-wave resonant interaction system [26,27], the self-induced transparency models [28], the long-wave–short-wave (LWSW) resonance [29–31], and the AB system [32,33]. Apart from the integrable situations, it has recently been shown that vector RWs can be excited in nonintegrable multicomponent systems arising from a quadratic medium [34]. More recently, the existence of multicomponent first- and second-order RWs (dark-dark type) have been experimentally demonstrated in a randomly birefringent telecom fiber [35,36].

Modulation instability (MI) is referred to as a basic process that the growth of perturbations emerges on an unstable continuous wave background [37]. In the explanation of the generation mechanism for RW, MI has been found to be closely linked with the RW excitation in nonlinear dispersive systems [35,38–41]. It has been shown that the RW modeled by the rational solution only exists in the subset of parameters where MI is present if and only if the unstable sideband spectrum also contains continuous-wave or zero-frequency perturbations as a limiting case [38,39]. In particular, it is known that RWs can only exist in focusing NLS equations; however, recent studies have shown that RWs can occur in coupled NLS equations of defocusing-defocusig type [38]. Besides, the evidence of passband and baseband polarization MIs in the defocusing Manakov system has been provided experimentally in optical fiber [35,42]. Therefore, we should study the vector RWs and their generation mechanism in various multicomponent systems both physically and mathematically.

In the 1970s, Benney first investigated in detail the interaction between the gravity wave (LW) and the capillary wave (SW) for the surface wave of deep water under certain resonance conditions [43] and then developed a general theory for

*junchaochen@aliyun.com

interactions between long and short waves [44]. Particularly, under the resonance condition, namely, the phase velocity of the LW is equal to the group velocity of the SW, energy exchange can be anticipated and the resonance interaction occurs [44]. Such resonance processes may occur in a variety of physical settings such as capillary-gravity waves, internal-surface waves, and short and long gravity waves on fluids of finite depth and the breakdown of laminar flow [44–47]. Benney proposed several coupled partial differential equations corresponding to various limiting situations connected with the relative magnitudes of dimensionless parameters which are ratios of wave amplitudes and length scales. Among which, there are two integrable cases: One is the Yajima-Oikawa system [45], and the other one is the Newell model [46,47]. Indeed, in the LWSW situation, the Yajima-Oikawa system is analogous to the NLS equation, whereas the Newell model is analogous to the derivative nonlinear Schrödinger (DNLS) equation [48].

So far, most of the studies for RW solutions are restricted to the NLS-type equations. In view of the mechanism for the formulation of RW and the actual situation for the occurrence of RW, i.e., the coexistence of gravity and capillary waves, it is imperative to study RWs in LWSW models in order to elucidate the formulation and interaction of rogue waves in more physical situations. Even though the RW solution for the LWSW model of Yajima-Oikawa type have been studied in the literature [29–31], as far as we are concerned, no RW solution is reported for the LWSW model of Newell type. Thus, it is worthwhile to investigate its RW solution from both the physical and mathematical points of view, which amounts to the motivation of the present work.

In the present paper, we first aim to construct the general RWs of the LWSW model of Newell type. Based on the general RWs in determinant form, we attempt to investigate the dynamics of first- and higher-order RWs and further to discuss the mechanism for the RW excitation through the MI analysis. The rest of this paper is organized as follows. In Sec. II, general higher-order rational solutions in terms of determinants with algebraic elements are derived via the Hirota's bilinear method and the KP hierarchy reduction. In Sec. III, local structures of RWs are analyzed and the results show that the SW possesses bright, intermediate, and dark patterns, whereas the LW always exhibits a bright state in the fundamental case. The higher-order RWs indicate the superposition of fundamental ones and they do not support interaction behaviors among different types of RW. In Sec. IV, MI analysis is carried out to find that the condition of the baseband MI coincides with the one for the existence of RW solutions. The present paper is concluded in Sec. V.

II. HIGH-ORDER RATIONAL SOLUTION IN DETERMINANT FORM

Based on Benney's theory [44] for the interaction between SW and LW, the integrable LWSW model of Newell type can be given by its gauge equivalent form [46–48]

$$iS_t + S_{xx} - 2iS_xL = 0, \tag{1}$$

$$L_t = -2\sigma(|S|^2)_x, \tag{2}$$

where $\sigma = \pm 1$, $S = S(x,t)$ represents the envelope of SW and $L = L(x,t)$ denotes the amplitude of LW. The general initial value problem for the model [(1) and (2)] was studied by Newell via the inverse scattering transform [47]. In fact, the spectral problem of such an integrable system corresponds to a deep reduction of three-wave resonance interaction [49]. The complete integrability of the LWSW model [(1) and (2)] was tested by Painlevé analysis [50]. Its Darboux transformation and the closed multisoliton solution formula have been constructed in Refs. [49,51]. The algebrogeometric and cusp solutions for this coupled system were provided in Refs. [52,53]. The different gauge equivalent versions of the LWSW model (1) and (2) were clarified in analogy with the DNLS equation, and their bright, dark soliton, and breather solutions with the uniform determinant form were derived via the Hirota's bilinear method [48].

By the dependent variable transformation

$$S = \rho e^{i\alpha(x-\alpha t)}\frac{g}{f^*}, \quad L = i\frac{\partial}{\partial x}\ln\frac{f^*}{f}, \tag{3}$$

where ρ and α are real parameters, the LWSW model (1) and (2) can be cast into the bilinear form

$$\left(iD_t + 2i\alpha D_x + D_x^2\right)g\cdot f = 0, \tag{4}$$

$$iD_tf\cdot f^* = D_x^2 f\cdot f^*, \tag{5}$$

$$iD_tf\cdot f^* = -2\sigma\rho^2(|f|^2 - |g|^2), \tag{6}$$

where f and g are complex variables, * denotes the complex conjugation, and D is Hirota's bilinear differential operator. Then we present the general Nth-order rational solutions in terms of the determinants of the LWSW model (1) and (2) in Theorem 1. This theorem and its proof are given in Appendix A.

III. DYNAMICS OF ROGUE-WAVE SOLUTIONS

A. Fundamental rogue wave

According to Theorem 1, in order to obtain the first-order RW, we need to take $N = 1$ in Eqs. (A1)–(A5). For simplicity, we set $a_0^{(0)} = 1$ and $a_1^{(0)} = 0$, and then the functions f and g are given by

$$f = \mu_0[(\hat{x} - \zeta_0)(\hat{x}^* + \zeta_0) + |\zeta_0|^2], \tag{7}$$

$$g = \mu_0\vartheta_0[(\hat{x} - \zeta_0 + \hat{\zeta}_0)(\hat{x}^* + \zeta_0 - \hat{\zeta}_0^*) + |\zeta_0|^2], \tag{8}$$

with $\hat{x} = \zeta(x + 2i\zeta t)$, $\zeta_0 = \frac{\zeta}{\zeta+\zeta^*}$, $\hat{\zeta}_0 = \frac{\zeta}{\zeta-i\alpha}$, $\vartheta_0 = -\frac{\zeta-i\alpha}{\zeta^*+i\alpha}$, and $\mu_0 = \frac{|\zeta-i\alpha|^2}{i\zeta(\zeta+\zeta^*)}e^{(\zeta+\zeta^*)[x-i(\zeta-\zeta^*)t]}$.

Then the fundamental RW solution for the LWSW model (1) and (2) reads

$$S = \rho\vartheta_0 e^{i\alpha(x-\alpha t)}\left[1 - \frac{\hat{\zeta}_0^*(\hat{x} - \zeta_0) - \zeta_0(\hat{x}^* + \hat{\zeta}_0) + |\hat{\zeta}_0|^2}{(\hat{x} - \zeta_0)(\hat{x}^* + \zeta_0) + |\zeta_0|^2}\right], \tag{9}$$

$$L = \frac{i(\zeta^*\hat{x}^2 - \zeta\hat{x}^{*2}) - i(\zeta_0 - \zeta_0^*)(\zeta^*\hat{x} + \zeta\hat{x}^*)}{|(\hat{x} - \zeta_0)(\hat{x}^* + \zeta_0) + |\zeta_0|^2|^2}. \tag{10}$$

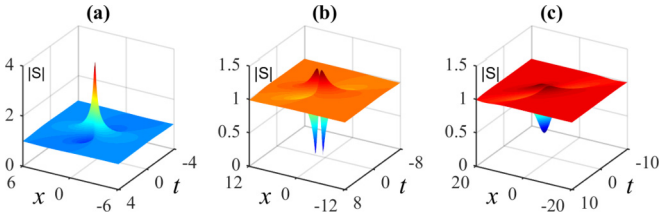

FIG. 1. First-order RW for SW in the LWSW model (1) and (2) with the parameters $\rho = -\sigma = 1$ and (a) bright state $\alpha = 1.5$; (b) intermediate state $\alpha = 2.1$ and (c) dark state $\alpha = 2.3$.

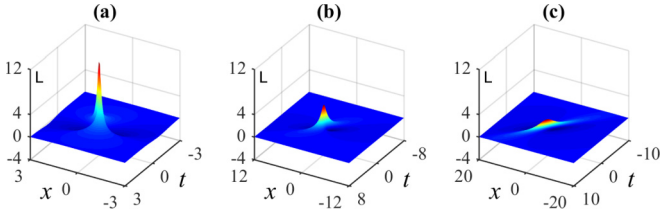

FIG. 2. First-order RW for LW in the LWSW model (1) and (2) with the parameters $\rho = -\sigma = 1$ and (a) $\alpha = 1.5$, (b) $\alpha = 2.1$, and (c) $\alpha = 2.3$, respectively.

Furthermore, the modular square of the SW component $|S|^2$ possesses extrema points: (x_1, t_1), $(x_2^{\pm}, t_2^{\pm})$, and $(x_3^{\pm}, t_3^{\pm})$ which are given by (B2)–(B4) in Appendix B. Note that $(x_2^{\pm}, t_2^{\pm})$ are two characteristic points, or zero-amplitude points, at which the amplitudes are zeros [29]. Through the local analysis, the fundamental RW for SW can be classified into three patterns: bright, intermediate and dark states. Without loss of generality, we take $\rho = 1$, and then there are two different cases ($\sigma = 1$ and $\sigma = -1$):

(I) In the case of $\sigma = 1$:

(a) Dark state ($0 < |\alpha| \leqslant \alpha_1^+$): two local maxima at $(x_3^{\pm}, t_3^{\pm})$ and one local minimum at (x_1, t_1). Especially, when $|\alpha| = \alpha_1^+$, the local minimum at the characteristic point $(x_1, t_1) = (x_2^{\pm}, t_2^{\pm})$.

(b) Intermediate state ($\alpha_1^+ < |\alpha| < \alpha_2^+$): two local maxima at $(x_3^{\pm}, t_3^{\pm})$ and two local minima at the characteristic point $(x_2^{\pm}, t_2^{\pm})$.

(c) Bright state ($\alpha_2^+ \leqslant |\alpha|$): one local maximum at (x_1, t_1) and two local minima at $(x_2^{\pm}, t_2^{\pm})$. When the sign takes "=", the local maximum at $(x_1, t_1) = (x_3^{\pm}, t_3^{\pm})$.

(II) In the case of $\sigma = -1$ ($0 < |\alpha| < \frac{3}{2}\sqrt{3}$ and $|\alpha| \neq \frac{\sqrt{2}}{2}$):

(a) Dark state ($\alpha_1^- \leqslant |\alpha| < \frac{3}{2}\sqrt{3}$): two local maxima at $(x_3^{\pm}, t_3^{\pm})$ and one local minimum at (x_1, t_1), especially, when $|\alpha| = \alpha_1^-$, the local minimum at the characteristic point $(x_1, t_1) = (x_2^{\pm}, t_2^{\pm})$.

(b) Intermediate state ($\alpha_2^- < |\alpha| < \alpha_1^-$): two local maxima at $(x_3^{\pm}, t_3^{\pm})$ and two local minima at the characteristic point $(x_2^{\pm}, t_2^{\pm})$.

(c) Bright state ($0 < |\alpha| \leqslant \alpha_2^-$): (i) $\frac{\sqrt{2}}{2} < |\alpha| \leqslant \alpha_2^-$: one local maximum at (x_1, t_1) and two local minima at $(x_2^{\pm}, t_2^{\pm})$; (ii) $0 < |\alpha| < \frac{\sqrt{2}}{2}$: one local maximum at (x_1, t_1) and two local minima at $(x_3^{\pm}, t_3^{\pm})$. When the sign takes "=", the local maximum at $(x_1, t_1) = (x_3^{\pm}, t_3^{\pm})$. Here the parameters are $\alpha_1^{\pm} = \frac{\sqrt{\mp 378 + 66\sqrt{33}}}{12}$ and $\alpha_2^{\pm} = \frac{\sqrt{\mp 18 + 6\sqrt{33}}}{4}$.

For the LW component L, it has extrema points (x_1, t_1) and $(x_4^{\pm}, t_4^{\pm})$, which are given by (B2) and (B5) in Appendix B. The further local analysis shows that in both cases $\sigma = \pm 1$, the RW of LW only exhibits the bright state with one local maximum at (x_1, t_1) and two local minima at $(x_4^{\pm}, t_4^{\pm})$.

As illustrated in Fig. 1, three types of RW depict different local structures of SW when the parameter α takes the value in its corresponding regimes. This implies that the RW's pattern for SW depends on α, which decides the number, the position, the height, and the type of extrema. Figure 2 displays the RW states of LW, and three cases correspond to the same parameters' choices as shown in Fig. 1. It can be clearly seen that as the value of α increases, the local structure of LW always features the bright RW and only the central amplitude decreases.

For the LWSW model (1) and (2), it can be viewed as a coupling extension of the DNLS equation, which is the Chen-Lee-Liu (CLL) equation. We recall that the DNLS equation only supports the RW of bright type with two zero-amplitude points. Here, due to the coupling component L which leads to complex interplay between the dispersion and the nonlinearity, dark and intermediate RWs appear for the SW component. From the local analysis, one can know that two kinds of bright RWs emerge under different parameters' conditions. Specifically, the normal bright RW with two characteristic points can be realized in the regions $|\alpha| \geqslant \alpha_1^+$ ($\sigma = 1$) and $\frac{\sqrt{2}}{2} < |\alpha| \leqslant \alpha_1^-$ ($\sigma = -1$). The other case ($|\alpha| < \frac{\sqrt{2}}{2}$ for $\sigma = -1$) corresponds to a special bright RW which also possesses one maximum and two minima amplitudes but two local minima are not characteristic points. More precisely, differing from the standard Peregrine soliton with the maximum amplitude as high as three times the background, the maximum amplitude of SW is α dependent and it can be calculated precisely as $A_b^{(S)} = |\frac{\zeta_1^2(\zeta_2 - 4\alpha) + \zeta_2(\zeta_2 - \alpha)^2}{\zeta_2[\zeta_1^2 + (\zeta_2 - \alpha)^2]}|$, which is plotted in Fig. 3 on the positive interval of α. One can see that for $\sigma = 1$, only as $\alpha \to +\infty$, the maximum amplitude approaches to three times the background. But for $\sigma = -1$, the maximum amplitude can reach infinity in the neighborhood of the singular point $\alpha = \frac{\sqrt{2}}{2}$. For the intermediate RW, it is always characterized by two local maxima and two local minima at zero-amplitude points. For the dark RW, its amplitude possesses two local maxima and one local minimum which usually cannot reach

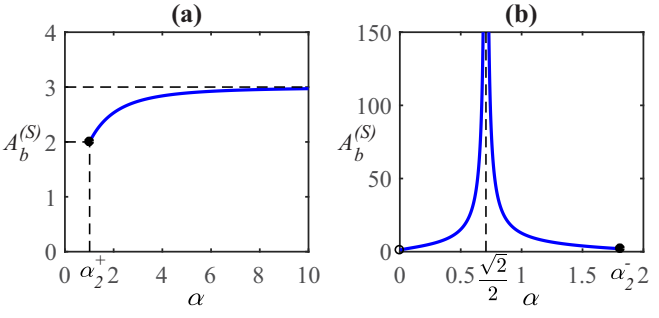

FIG. 3. The maximum amplitude of the bright RW for SW in the LWSW model (1) and (2) with the parameters $\rho = 1$ and (a) $\sigma = 1$ and (b) $\sigma = -1$.

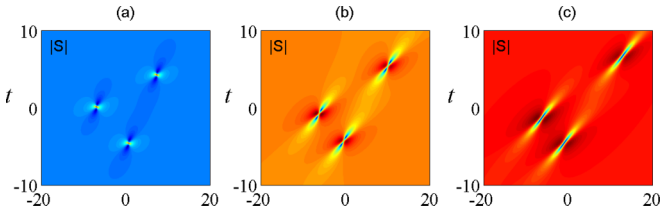

FIG. 4. Second-order RW for SW in the LWSW model (1) and (2) with the parameters $\rho = -\sigma = 1$, $a_0^{(0)} = 1, a_1^{(0)} = a_2^{(0)} = 0, a_3^{(0)} = 350$ and (a) bright state $\alpha = 1.5$, (b) intermediate state $\alpha = 2.1$, and (c) dark state $\alpha = 2.3$.

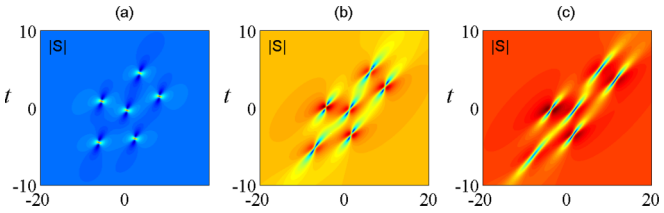

FIG. 5. Third-order RW for SW in the LWSW model (1) and (2) with the parameters $\rho = -\sigma = 1$, $a_0^{(0)} = 1, a_1^{(0)} = a_2^{(0)} = a_3^{(0)} = a_4^{(0)} = 0, a_5^{(0)} = 2000$ and (a) bright state $\alpha = 1.5$, (b) intermediate state $\alpha = 2.1$, and (c) dark state $\alpha = 2.3$.

zero. However, at the critical case between the dark RW and the intermediate one in which α takes $|\alpha| = \alpha_1^{\pm}$, the local minimum occurs at zero-amplitude points. In this situation, the dark RW reduces to a special one which is referred to as a black RW.

B. High-order rogue wave

The second-order RW solution is obtained from Eqs. (A1)–(A3) with $N = 2$. In this case, setting $a_0^{(0)} = 1$, $a_1^{(0)} = a_2^{(0)} = 0$, we obtain the functions f and g as follows:

$$f = \begin{vmatrix} m_{11}^{(1,1,-1,0)} & m_{13}^{(1,0,-1,0)} \\ m_{31}^{(0,1,-1,0)} & m_{33}^{(0,0,-1,0)} \end{vmatrix}, \quad g = \begin{vmatrix} m_{11}^{(1,1,-1,1)} & m_{13}^{(1,0,-1,1)} \\ m_{31}^{(0,1,-1,1)} & m_{33}^{(0,0,-1,1)} \end{vmatrix}, \tag{11}$$

where the elements are determined by

$$\begin{aligned} m_{11}^{(1,1,n,k)} &= A_1^{(1)} B_1^{(1)} m^{(n,k)}\big|_{p=\zeta, q=\zeta^*}, \\ m_{13}^{(1,0,n,k)} &= A_1^{(1)} B_3^{(0)} m^{(n,k)}\big|_{p=\zeta, q=\zeta^*}, \\ m_{31}^{(0,1,n,k)} &= A_3^{(0)} B_1^{(1)} m^{(n,k)}\big|_{p=\zeta, q=\zeta^*}, \\ m_{33}^{(0,0,n,k)} &= A_3^{(0)} B_3^{(0)} m^{(n,k)}\big|_{p=\zeta, q=\zeta^*}, \end{aligned}$$

and the differential operators $A_1^{(1)} = a_0^{(1)}(p - i\alpha)\partial_p + a_1^{(1)}$, $B_1^{(1)} = a_0^{(1)*}(q + i\alpha)\partial_q + a_1^{(1)*}$, $A_3^{(0)} = \frac{1}{6}[(p - i\alpha)\partial_p]^3 + a_3^{(0)}$, $B_3^{(0)} = \frac{1}{6}[(q + i\alpha)\partial_q]^3 + a_3^{(0)*}$ with $a_0^{(1)} = 2(p - i\alpha)^2 + \frac{i\sigma\alpha\rho^2}{p - i\alpha} + i\alpha(p - i\alpha)$ and $a_1^{(1)} = \frac{1}{3}[4(p - i\alpha)^2 - \frac{i\sigma\alpha\rho^2}{p - i\alpha} + i\alpha(p - i\alpha)]$.

Since the LW always features a bright RW, we only present the configuration of SW to illustrate the higher RWs. Three second-order RWs for SW are displayed in Fig. 4, each one takes the same value of the parameter α as one shown in Fig. 1. One can see that second-order RWs manifest the superposition of three fundamental ones and they obey the triangle arrays. Due to the same parameters α as the first-order cases, respectively, three second-order RWs display purely dark, intermediate, and bright RW's combinations individually.

For third- and higher-order RWs, which describe the superposition of more fundamental RWs, one needs to take larger N in (A1)–(A5). The expressions are too complicated to be listed here. Figure 5 shows the third-order RW for $N = 3$ graphically, in which three plots still take the same parameter α as in Figs. 1 and 4. It can be seen that third-order RWs describe the superposition of six fundamental ones and they constitute a shape of pentagon. Besides, each combination only contains one type of elementary RW purely in three cases, which agrees with ones of first- and second-order cases. This fact suggests that only three types of RW for SW happen in both fundamental and higher-order cases and the RW's pattern completely depends on the parameter α. For instance, when $\sigma = 1$, three types of RW (the fundamental one and the higher-order superposition) strictly occur at three intervals of the structural parameter α, i.e., $|\alpha| \leqslant \alpha_1^+$ for the dark state, $\alpha_1^+ < |\alpha| < \alpha_2^+$ for the intermediate state, and $|\alpha| \geqslant \alpha_2^+$ for the bright state. That is, the construction of higher-order RW solutions here do not allow the mixed superposition among different types of fundamental RWs.

As seen in Figs. 1, 4 and 5 for first-, second- and third-order RWs of SW, an Nth-order RW can evolve into at most $N(N + 1)/2$ fundamental RWs. Indeed, apart from the structural parameter α, an Nth-order RW in the LWSW model (1) and (2) contains N free complex parameters $a_{2i-1}^{(0)} (i = 1, \ldots, N)$ as reported in Ref. [17]. These parameters determine the arrangement of $N(N + 1)/2$ fundamental RWs for the given Nth-order RW, which means that rich spatiotemporal patterns can be obtained under different choices of free parameters. In particular, it is known that Nth-order RW can reach a climax of $2N + 1$ times the background height by a specific choice of parameters in scalar NLS equation [13]. However, the coupled system (1) and (2) has different cases for $\sigma = 1$ and $\sigma = -1$, respectively. For $\sigma = 1$, as shown in Fig. 3(a) for the first-order bright RW of SW, only as $\alpha \to \infty$, the maximum amplitude approaches to three times the background. Correspondingly, each peaks in Nth-order RW can come together and form a single main lump with the maximum amplitude by a special choice of free parameters. But this maximum amplitude might not be $2N + 1$ times the background except for $\alpha \to \infty$. This kind of special RW is depicted in Fig. 6 for bright RWs of SW with the

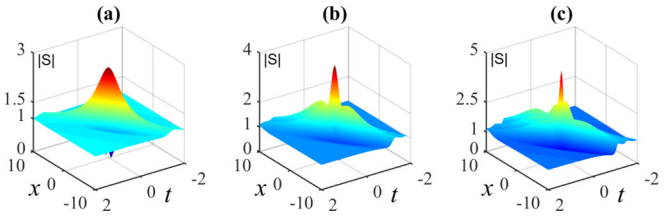

FIG. 6. Bright RWs with single main hump for SW in the LWSW model (1) and (2) given by the parameters $\rho = \sigma = a_0^{(0)} = 1, a_2^{(0)} = a_4^{(0)} = 0$, $\alpha = 3$: (a) first-order case, (b) second-order case, and (c) third-order case.

parameters: (a) first-order case $a_1^{(0)} = 0.4380 + 0.2057i$; (b) second-order case $a_1^{(0)} = 0.3653 + 0.3210i$ and $a_3^{(0)} = -0.0253 + 0.0343i$; and (c) third-order case $a_1^{(0)} = 0.2926 + 0.4363i$, $a_3^{(0)} = -0.0076 + 0.0277i$, and $a_5^{(0)} = 0.0010 + 0.0027i$. For $\sigma = -1$, as displayed in Fig. 3(b), the maximum amplitude only for the first-order bright RW can reach infinity near the singular point. Thus the higher-order RW in this case cannot support a super RW through the specific choice of parameters.

IV. MODULATION INSTABILITY

Next we investigate the linear stability analysis of the plane-wave background solutions of the LWSW model by considering small perturbations of the form $S = [a + S_1]e^{i[\omega x - (\omega^2 - 2b\omega)t]}$ and $L = b + L_1$, where S_1 and L_1 are small complex perturbations. The substitution yields a group of linearized partial differential equations. Recalling that L is real, we can assume the perturbations are space periodic with the fixed frequency Ω, i.e., $S_1 = s_1(t)e^{i\Omega x} + s_2(t)e^{-i\Omega x}$ and $L_1 = l(t)e^{i\Omega x} + l^*(t)e^{-i\Omega x}$, which leads the above linearized partial differential equations into a group of linear ordinary differential equations $s' = iMs$ with $s = [s_1, s_2^*, l]^T$ and

$$M = \begin{bmatrix} -\Omega^2 + 2b\Omega - 2\omega\Omega & 0 & 2a\omega \\ 0 & \Omega^2 + 2b\Omega - 2\omega\Omega & -2a\omega \\ -2a\sigma\Omega & -2a\sigma\Omega & 0 \end{bmatrix}. \tag{12}$$

This set of differential equations with the real frequency Ω suggests that the functions $s_1(t)$, $s_2(t)$, and $l(t)$ are the linear combinations of exponentials $\exp(i\lambda_j t)$, where λ_j, $j = 1, 2, 3$ represent three eigenvalues of the matrix M. Such eigenvalues are given by the roots of the characteristic polynomial $P(\lambda)$ of the matrix M,

$$P(\lambda) = \lambda^3 + P_2\lambda^2 + P_1\lambda + P_0, \tag{13}$$

with $P_2 = 4(\omega - b)\Omega$, $P_1 = [4(b - \omega)^2 - \Omega^2]\Omega^2$, and $P_0 = -8\sigma\omega a^2\Omega^3$.

It is known that when an eigenvalue of M has a negative imaginary part, MI will occur with the exponential growing perturbation. From the matrix M, one can see that each entry is real, so the corresponding eigenvalues are either real root or a pair of complex-conjugate roots. More specifically, we calculate the discriminant of the characteristic polynomial $P(\lambda)$ as

$$\Delta = 4\Omega^6\{3\Omega^6 - 24(b - \omega)^2\Omega^4 - 48(b - \omega)[9\sigma\omega a^2 - (b - \omega)^3]\Omega^2 - 48\sigma\omega a^2[27\sigma\omega a^2 - 4(b - \omega)^3]\}. \tag{14}$$

Then $\Delta > 0$ results in real roots for the polynomial $P(\lambda)$, which implies that no MI appears, whereas $\Delta < 0$ yields two complex conjugate roots, which implies that MI exists. The marginal stability curve corresponds to the discriminant $\Delta = 0$. Thus the plane-wave background solutions $S = e^{i[\omega x - (\omega^2 - 2b\omega)t]}$ and $L = b$ are modulationally unstable with $\Delta < 0$, which suggests that the RW solutions given by the transformation (3) with the background amplitudes $a = \rho$ and $b = 0$ are unstable in the LWSW model (1) and (2). Without loss of generality, by taking $a = 1$ and $b = 0$, MI gain spectrums are displayed for two kinds of nonlinearity $\sigma = 1$ and $\sigma = -1$ in Fig. 7, respectively.

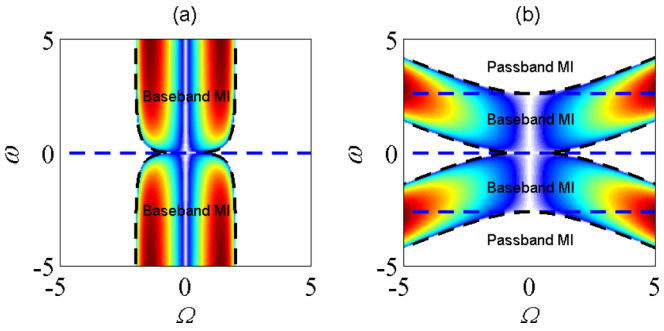

FIG. 7. MI for the LWSW model (1) and (2) on the (Ω, ω) plane calculated with the parameters $a = 1$, $b = 0$, and (a) $\sigma = 1$ and (b) $\sigma = -1$. Dark dashed curves indicate the analytical marginal stability condition $\Delta = 0$.

As analyzed in Refs. [38,39], baseband MI defined as the condition where an unstable continuous-wave background corresponds to perturbations infinitesimally small frequencies is responsible for the RW excitation, whereas passband MI, which means the perturbation undergoes gain in a spectral region not including zero frequency as a limiting case, does not support RW. Thus baseband MI is usually a certain subset of the parameters ω and Ω where MI is present. Figure 7(a) shows the MI gain for $\sigma = 1$; this MI is of baseband type except for $\omega \neq 0$. But in Fig. 7(b) for $\sigma = -1$, there exist regions of either baseband or passband MI. The limit situation where $\Omega \to 0$ determines the occurrence of baseband MI. In this case, the discriminant of the polynomial $P(\lambda)$ degenerates to $\Delta = -48\sigma\omega(4\omega^3 + 27\sigma\omega)$, which gives rise to two cases: (1) $\sigma = 1$, $\Delta < 0$ means that the baseband MI is always present except for $\omega \neq 0$ [see Fig. 7(a)] and (2) $\sigma = -1$, $\Delta < 0$ leads to the baseband MI condition: $0 < |\omega| < \frac{3}{2}\sqrt{3}$ [see Fig. 7(b)]. The coincidence is that the baseband MI condition is exactly the one for the existence of RW solutions.

V. CONCLUSION

The general higher-order rational solutions of the LWSW model are derived via the Hirota's bilinear method and the KP hierarchy reduction. These explicit solutions in terms of determinants with algebraic elements depict the fundamental and higher-order RWs. It is found that the fundamental RW of SW contains three different patterns: bright, intermediate, and dark states, whereas the RW of LW is always a bright state. The higher-order RWs indicate the superposition of fundamental ones and they do not support interaction behaviors among different types of RW. The MI analysis shows that the condition of the baseband MI where an unstable plane-wave background corresponds to perturbations with infinitesimally small frequencies coincides with the condition for the existence of RW solutions.

ACKNOWLEDGMENTS

J.C. expresses his sincere thanks to Profs. L. Ling, J. Yang, and Y. Ohta for their enthusiastic support and useful

suggestions. J.C. acknowledges the support from NSF of China (Grant No.11705077). B.-F. acknowledges the partial support from NSF (Grant No. DMS-1715991) and NSF of China (Grant No. 11728103). K.M.'s work was supported by JSPS Grant-in-Aid for Scientific Research (Grant No. C-15K04909) and JST CREST.

APPENDIX A

In this Appendix, we list the theorem on the general Nth-order rational solutions of the LWSW model (1) and (2) and prove this theorem via the KP hierarchy reduction method.

Theorem 1. The LWSW equations (1) and (2) have the rational solutions (3) with the tau functions f and g given by $N \times N$ determinants

$$f = \tau_{-1,0}, \quad g = \tau_{-1,1}, \tag{A1}$$

where $\tau_{n,k} = \det_{1\leqslant i,j\leqslant N}(m_{2i-1,2j-1}^{(N-i,N-j,n,k)})$ and the matrix elements are defined by

$$m_{i,j}^{(\nu,\mu,n,k)} = \sum_{l=0}^{i}\sum_{s=0}^{j}\frac{a_l^{(\nu)}}{(i-l)!}\frac{a_s^{(\mu)*}}{(j-s)!}[(p-i\alpha)\partial_p]^{i-l}[(q+i\alpha)\partial_q]^{j-s}m^{(n,k)}\Big|_{p=\zeta,q=\zeta^*}, \tag{A2}$$

with

$$m^{(n,k)} = \frac{ip}{p+q}\left(-\frac{p}{q}\right)^n\left(-\frac{p-i\alpha}{q+i\alpha}\right)^k e^{(p+q)x-(p^2-q^2)it}, \tag{A3}$$

$$a_l^{(\nu+1)} = \sum_{j=0}^{l}\frac{1}{(j+2)!}\left[2^{j+2}(p-i\alpha)^2 + (-1)^j\frac{2i\sigma\alpha\rho^2}{p-i\alpha} + 2i\alpha(p-i\alpha)\right]a_{l-j}^{(\nu)}, \quad \nu = 0, 1, 2, \ldots, \tag{A4}$$

and ζ need to satisfy the relation

$$2\zeta - \frac{2\sigma i\alpha\rho^2}{(\zeta - i\alpha)^2} = 0. \tag{A5}$$

Proof. First, we present the following lemma.

Lemma 1. The bilinear equations in the extended KP hierarchy

$$\left(D_{x_2} - 2aD_{x_1} - D_{x_1}^2\right)\tau_{n,k+1}\cdot\tau_{n,k} = 0, \tag{A6}$$

$$\left(D_{x_2} + D_{x_1}^2\right)\tau_{n,k}\cdot\tau_{n+1,k} = 0, \tag{A7}$$

$$\left(aD_{t_a} + 1\right)\tau_{n,k}\cdot\tau_{n+1,k} = \tau_{n,k+1}\tau_{n+1,k-1}, \tag{A8}$$

where a is a complex constant and n and k are integers and have the following solution:

$$\tau_{n,k} = \tilde{m}^{(n,k)} = \frac{ip}{p+q}\left(-\frac{p}{q}\right)^n\left(-\frac{p-a}{q+a}\right)^k e^{\tilde{\xi}+\tilde{\eta}}, \tag{A9}$$

with

$$\tilde{\xi} = \frac{1}{p-a}t_a + px_1 + p^2x_2, \quad \tilde{\eta} = \frac{1}{q+a}t_a + qx_1 - q^2x_2,$$

where p, q, and a are complex parameters.

In order to derive the rational solution, we introduce the differential operators $A_k^{(\nu)}$ and $B_l^{(\mu)}$ with respect to p and q, respectively,

$$A_n^{(\nu)} = \sum_{k=0}^{n}a_k^{(\nu)}\frac{[(p-a)\partial_p]^{n-k}}{(n-k)!}, \quad n \geqslant 0, \tag{A10}$$

$$B_n^{(\nu)} = \sum_{k=0}^{n}b_k^{(\nu)}\frac{[(q+a)\partial_q]^{n-k}}{(n-k)!}, \quad n \geqslant 0, \tag{A11}$$

where $a_k^{(\nu)}$ and $b_k^{(\nu)}$ are constants satisfying the iterated relations

$$a_k^{(\nu+1)} = \sum_{j=0}^{k} \frac{2^{j+2}(p-a)^2 + (-1)^j \frac{\lambda a}{p-a} + 2a(p-a)}{(j+2)!} a_{k-j}^{(\nu)}, \quad \nu = 0, 1, 2, \ldots, \tag{A12}$$

$$b_k^{(\nu+1)} = \sum_{j=0}^{k} \frac{2^{j+2}(q+a)^2 - (-1)^j \frac{\lambda a}{q+a} - 2a(q+a)}{(j+2)!} b_{k-j}^{(\nu)}, \quad \nu = 0, 1, 2, \ldots . \tag{A13}$$

Based on the Leibniz rule, one has

$$[(p-a)\partial_p]^m \left(p^2 + \frac{\lambda a}{p-a}\right) = \sum_{l=0}^{m} \binom{m}{l} \left[2^l (p-a)^2 + (-1)^l \frac{\lambda a}{p-a} + 2a(p-a)\right] [(p-a)\partial_p]^{m-l} + a^2 [(p-a)\partial_p]^m \tag{A14}$$

and

$$[(q+a)\partial_q]^m \left(q^2 - \frac{\lambda a}{q+a}\right) = \sum_{l=0}^{m} \binom{m}{l} \left[2^l (q+a)^2 - (-1)^l \frac{\lambda a}{q+a} - 2a(q+a)\right] [(q+a)\partial_q]^{m-l} + a^2 [(q+a)\partial_q]^m. \tag{A15}$$

Furthermore, we can derive

$$\begin{aligned}
\left[A_n^{(\nu)}, p^2 + \frac{\lambda a}{p-a}\right] &= \sum_{k=0}^{n-1} \frac{a_k^{(\nu)}}{(n-k)!} \left[((p-a)\partial_p)^{n-k}, p^2 + \frac{\lambda a}{p-a}\right] \\
&= \sum_{k=0}^{n-1} \frac{a_k^{(\nu)}}{(n-k)!} \sum_{l=1}^{n-k} \binom{n-k}{l} \left(2^l (p-a)^2 + (-1)^l \frac{\lambda a}{p-a} + 2a(p-a)\right) ((p-a)\partial_p)^{n-k-l},
\end{aligned}$$

where $[\,,\,]$ is the commutator defined by $[X, Y] = XY - YX$.

Let $\tilde{\zeta}$ be the solution of the algebraic equation

$$2p - \frac{\lambda a}{(p-a)^2} = 0.$$

Hence we have

$$\left[A_n^{(\nu)}, p^2 + \frac{\lambda a}{p-a}\right]\Big|_{p=\tilde{\zeta}} = 0,$$

for $n = 0, 1$ and

$$\begin{aligned}
&\left[A_n^{(\nu)}, p^2 + \frac{\lambda a}{p-a}\right]\Big|_{p=\tilde{\zeta}} \\
&= \sum_{k=0}^{n-2} \frac{a_k^{(\nu)}}{(n-k)!} \sum_{l=2}^{n-k} \binom{n-k}{l} \left\{2^l (p-a)^2 + (-1)^l \frac{\lambda a}{p-a} + 2a(p-a)\right\} [(p-a)\partial_p]^{n-k-l} \Big|_{p=\tilde{\zeta}} \\
&= \sum_{k=0}^{n-2} \sum_{j=0}^{n-k-2} \frac{a_k^{(\nu)}}{(j+2)!(n-k-j-2)!} \left\{2^{j+2}(p-a)^2 + (-1)^j \frac{\lambda a}{p-a} + 2a(p-a)\right\} [(p-a)\partial_p]^{n-k-j-2} \Big|_{p=\tilde{\zeta}} \\
&= \sum_{\hat{k}=0}^{n-2} \left[\sum_{\hat{j}=0}^{\hat{k}} \frac{2^{\hat{j}+2}(p-a)^2 + (-1)^{\hat{j}} \frac{\lambda a}{p-a} + 2a(p-a)}{(\hat{j}+2)!} a_{\hat{k}-\hat{j}}^{(\nu)}\right] \frac{[(p-a)\partial_p]^{n-2-\hat{k}}}{(n-2-\hat{k})!} \Big|_{p=\tilde{\zeta}} \\
&= \sum_{\hat{k}=0}^{n-2} a_{\hat{k}}^{(\nu+1)} \frac{[(p-a)\partial_p]^{n-2-\hat{k}}}{(n-2-\hat{k})!} \Big|_{p=\tilde{\zeta}} \\
&= A_{n-2}^{(\nu+1)}\big|_{p=\tilde{\zeta}},
\end{aligned}$$

for $n \geqslant 2$. Thus the differential operator $A_n^{(\nu)}$ satisfies the following relation:

$$\left[A_n^{(\nu)}, p^2 + \frac{2i}{p-a}\right]\Big|_{p=\tilde{\zeta}} = A_{n-2}^{(\nu+1)}\big|_{p=\tilde{\zeta}}, \tag{A16}$$

where we define $A_n^{(\nu)} = 0$ for $n < 0$.

Similarly, it is shown that the differential operator $B_n^{(\nu)}$ satisfies

$$\left[B_n^{(\nu)}, q^2 - \frac{\lambda a}{q+a}\right]\Big|_{q=\bar{\bar{\xi}}} = B_{n-2}^{(\nu+1)}\big|_{q=\bar{\bar{\xi}}}, \tag{A17}$$

where we define $B_n^{(\nu)} = 0$ for $n < 0$ and $\bar{\bar{\xi}}$ needs to satisfy

$$2q + \frac{\lambda a}{(q+a)^2} = 0. \tag{A18}$$

Consequently, by referring to the above two relations (A16) and (A17), we have

$$\begin{aligned}
\left(\partial_{x_2} + \lambda a \partial_{t_a}\right)\tilde{m}_{ls}^{(\nu,\mu,n,k)}\big|_{p=\tilde{\zeta},q=\bar{\bar{\xi}}} &= \left[A_l^{(\nu)} B_s^{(\mu)}\left(\partial_{x_2} + \lambda a \partial_{t_a}\right)\tilde{m}^{(n,k)}\right]\big|_{p=\tilde{\zeta},q=\bar{\bar{\xi}}} \\
&= \left\{A_l^{(\nu)} B_s^{(\mu)}\left[p^2 - q^2 + \lambda a\left(\frac{1}{p-a} + \frac{1}{q+a}\right)\right]\tilde{m}^{(n)}\right\}\Big|_{p=\tilde{\zeta},q=\bar{\bar{\xi}}} \\
&= \left[A_l^{(\nu)}\left(p^2 + \frac{\lambda a}{p-a}\right)B_s^{(\mu)}\tilde{m}^{(n)}\right]\Big|_{p=\tilde{\zeta},q=\bar{\bar{\xi}}} - \left[A_l^{(\nu)} B_s^{(\mu)}\left(q^2 - \frac{\lambda a}{q+a}\right)\tilde{m}^{(n)}\right]\Big|_{p=\tilde{\zeta},q=\bar{\bar{\xi}}} \\
&= \left\{\left[\left(p^2 + \frac{\lambda a}{p-a}\right)A_l(\nu) + A_{l-2}^{(\nu+1)}\right]B_s^{(\mu)}\tilde{m}^{(n,k)}\right\}\Big|_{p=\tilde{\zeta},q=\bar{\bar{\xi}}} \\
&\quad - \left\{A_l^{(\nu)}\left[\left(q^2 - \frac{\lambda a}{q+a}\right)B_s^{(\mu)} + B_{s-2}^{(\mu+1)}\right]\tilde{m}^{(n,k)}\right\}\Big|_{p=\tilde{\zeta},q=\bar{\bar{\xi}}} \\
&= \left(\tilde{\zeta}^2 + \frac{\lambda a}{\tilde{\zeta}-a}\right)\tilde{m}_{ls}^{(\nu,\mu,n,k)}\big|_{p=\tilde{\zeta},q=\bar{\bar{\xi}}} + \tilde{m}_{l-2,s}^{(\nu+1,\mu,n,k)}\big|_{p=\tilde{\zeta},q=\bar{\bar{\xi}}} \\
&\quad - \left(\bar{\bar{\xi}}^2 - \frac{\lambda a}{\bar{\bar{\xi}}+a}\right)\tilde{m}_{ls}^{(\nu,\mu,n,k)}\big|_{p=\tilde{\zeta},q=\bar{\bar{\xi}}} - \tilde{m}_{l,s-2}^{(\nu,\mu+1,n,k)}\big|_{p=\tilde{\zeta},q=\bar{\bar{\xi}}}.
\end{aligned}$$

Then the differential of the following determinant:

$$\tilde{\tau}_{n,k} = \det_{1\leqslant i,j\leqslant N}\left(\tilde{m}_{2i-1,2j-1}^{(N-i,N-j,n,k)}\big|_{p=\tilde{\zeta},q=\bar{\bar{\xi}}}\right)$$

can be calculated as

$$\begin{aligned}
\left(\partial_{x_2} + \lambda a \partial_{t_a}\right)\tilde{\tau}_n &= \sum_{i=1}^{N}\sum_{j=1}^{N}\Delta_{ij}\left(\partial_{x_2} + \lambda a \partial_{t_a}\right)\left[\tilde{m}_{2i-1,2j-1}^{(N-i,N-j,n,k)}\big|_{p=\tilde{\zeta},q=\bar{\bar{\xi}}}\right] \\
&= \sum_{i=1}^{N}\sum_{j=1}^{N}\Delta_{ij}\left[\left(\tilde{\zeta}^2 + \frac{\lambda a}{\tilde{\zeta}-a}\right)\tilde{m}_{2i-1,2j-1}^{(N-i,N-j,n,k)}\big|_{p=\tilde{\zeta},q=\bar{\bar{\xi}}} + \tilde{m}_{2i-3,2j-1}^{(N-i+1,N-j,n,k)}\big|_{p=\tilde{\zeta},q=\bar{\bar{\xi}}}\right. \\
&\quad \left. - \left(\bar{\bar{\xi}}^2 - \frac{\lambda a}{\bar{\bar{\xi}}+a}\right)\tilde{m}_{2i-1,2j-1}^{(N-i,N-j,n,k)}\big|_{p=\tilde{\zeta},q=\bar{\bar{\xi}}} - \tilde{m}_{2i-1,2j-3}^{(N-i,N-j+1,n,k)}\big|_{p=\tilde{\zeta},q=\bar{\bar{\xi}}}\right] \\
&= \left(\tilde{\zeta}^2 + \frac{\lambda a}{\tilde{\zeta}-a}\right)N\tilde{\tau}_n + \sum_{i=1}^{N}\sum_{j=1}^{N}\Delta_{ij}\tilde{m}_{2i-3,2j-1}^{(N-i+1,N-j,n,k)}\big|_{p=\tilde{\zeta},q=\bar{\bar{\xi}}} \\
&\quad - \left(\bar{\bar{\xi}}^2 - \frac{\lambda a}{\bar{\bar{\xi}}+a}\right)N\tilde{\tau}_n - \sum_{i=1}^{N}\sum_{j=1}^{N}\Delta_{ij}\tilde{m}_{2i-1,2j-3}^{(N-i,N-j+1,n,k)}\big|_{p=\tilde{\zeta},q=\bar{\bar{\xi}}},
\end{aligned}$$

where Δ_{ij} is the (i, j) cofactor of the matrix $[\tilde{m}_{2i-1,2j-1}^{(N-i,N-j,n)}|_{p=\tilde{\zeta},q=\bar{\bar{\xi}}}]_{1\leqslant i,j\leqslant N}$. For the term $\sum_{i=1}^{N}\sum_{j=1}^{N}\Delta_{ij}\tilde{m}_{2i-3,2j-1}^{(N-i+1,N-j,n)}|_{p=\tilde{\zeta},q=\bar{\bar{\xi}}}$, it vanishes since for $i = 1$ this summation is a determinant with the elements in first row being zero and for $i = 2, 3, \ldots$ this summation is a determinant with two identical rows. Similarly, the term $\sum_{i=1}^{N}\sum_{j=1}^{N}\Delta_{ij}\tilde{m}_{2i-1,2j-3}^{(N-i,N-j+1,n)}|_{p=\tilde{\zeta},q=\bar{\bar{\xi}}}$ vanishes. Therefore, $\tilde{\tau}_n$ satisfies the reduction condition

$$\left(\partial_{x_2} + \lambda a \partial_{t_a}\right)\tilde{\tau}_n = \left(\tilde{\zeta}^2 - \bar{\bar{\xi}}^2 + \frac{\lambda a}{\tilde{\zeta}-a} + \frac{\lambda a}{\bar{\bar{\xi}}+a}\right)N\tilde{\tau}_n, \tag{A19}$$

such that these algebraic solutions $\tilde{\tau}_{n,k}$ satisfy the $(1+1)$-dimensional bilinear equations:

$$\left(D_{x_2} - 2aD_{x_1} - D_{x_1}^2\right)\tilde{\tau}_{n,k+1}\cdot\tilde{\tau}_{n,k} = 0, \tag{A20}$$

$$\left(D_{x_2} + D_{x_1}^2\right)\tilde{\tau}_{n,k}\cdot\tilde{\tau}_{n+1,k} = 0, \tag{A21}$$

$$D_{x_2}\tilde{\tau}_{n,k}\cdot\tilde{\tau}_{n+1,k} = \lambda(\tilde{\tau}_{n,k}\tilde{\tau}_{n+1,k} - \tilde{\tau}_{n,k+1}\tilde{\tau}_{n+1,k-1}). \tag{A22}$$

By taking $a = i\alpha$, $\lambda = 2\sigma\rho^2$, $\tilde{\bar{\zeta}} = \tilde{\zeta}^*$, and $x_1 = x$, $x_2 = it$, one can define

$$f = \tau_{-1,0},\quad g = \tau_{-1,1},\quad f^* = \tau_{0,0},\quad g^* = \tau_{0,-1}. \tag{A23}$$

which reduce (A20)–(A22) to the bilinear equations (4)–(6). From the reduction condition (A19), t_a becomes a dummy variable which can be taken as zero. Therefore we arrive at Theorem 1.

APPENDIX B

Let $\zeta = \zeta_1 + i\zeta_2$ in Eq. (A5), where ζ_1 and ζ_2 are real and imaginary parts, respectively, and they can be expressed explicitly by

$$\zeta_1 = \frac{\sqrt{3}(\Lambda^2 - 4\alpha^2)}{12\delta_1\Lambda},\quad \zeta_2 = \frac{2}{3}\alpha + \frac{1}{12}\Lambda + \frac{\alpha^2}{3\Lambda}, \tag{B1}$$

with $\Lambda = [4\alpha(2\alpha^2 + 27\sigma\rho^2) + 12\delta_2\alpha\rho\sqrt{3(4\sigma\alpha^2 + 27\rho^2)}]^{1/3}$ and $\delta_1, \delta_2 = \pm 1$. Thus the RW solutions exist under the constraints: $4\sigma\alpha^2 + 27\rho^2 > 0$ and $\alpha \neq 0$, namely $\alpha \neq 0$ for $\sigma = 1$ and $0 < |\alpha| < \frac{3}{2}\sqrt{3}|\rho|$ for $\sigma = -1$, respectively. Further the modular square of the first-order RW for the SW component (9) possesses extrema points (turning points where the first derivatives vanish):

$$(x_1, t_1) \equiv \left[\frac{\zeta_2^2}{\zeta_1\left(\zeta_1^2 + \zeta_2^2\right)}, \frac{1}{4}\frac{\zeta_2}{\zeta_1\left(\zeta_1^2 + \zeta_2^2\right)}\right], \tag{B2}$$

$$(x_2^{\pm}, t_2^{\pm}) \equiv \left[\frac{\zeta_2\left(\alpha^2 - \zeta_1^2 - \zeta_2^2\right)}{2\zeta_1\Delta_3} - \frac{2\Delta_5\mu_1}{\Delta_1\Delta_3\zeta_1^2}, \frac{\mu_1}{\Delta_1\zeta_1^2}\right], \tag{B3}$$

$$(x_3^{\pm}, t_3^{\pm}) \equiv \left[-\frac{\zeta_2\left(\alpha^2 - \zeta_1^2 - \zeta_2^2\right)}{2\zeta_1\Delta_6} + \frac{2\Delta_7\mu_2}{\Delta_1\Delta_6\zeta_1}, \frac{\mu_2}{\Delta_1\zeta_1^2}\right], \tag{B4}$$

and the first-order RW for the LW component (10) has extrema points: (x_1, t_1) and

$$(x_4^{\pm}, t_4^{\pm}) \equiv \left[\frac{2\left(\zeta_1^2 + 3\zeta_2^2\right)}{\zeta_1}\mu_3 - \frac{1}{2\zeta_1}, \frac{\zeta_2}{\zeta_1}\mu_3\right], \tag{B5}$$

with $\mu_1 = \frac{\zeta_1\zeta_2\Delta_1}{4(\zeta_1^2+\zeta_2^2)} \pm \frac{\sqrt{-\zeta_2\Delta_2\Delta_3^2\Delta_4}}{4(\zeta_1^2+\zeta_2^2)\Delta_2}$, $\mu_2 = \frac{\zeta_2\Delta_1}{4(\zeta_1^2+\zeta_2^2)} \pm \frac{\sqrt{\zeta_2\Delta_6^2\Delta_8\Delta_9}}{4(\zeta_1^2+\zeta_2^2)\Delta_9}$, $\mu_3 = \frac{1}{4(\zeta_1^2+\zeta_2^2)} \pm \frac{\sqrt{3}}{4}\frac{\sqrt{\zeta_2^2(\zeta_1^2+4\zeta_2^2)}}{(\zeta_1^2+\zeta_2^2)(\zeta_1^2+4\zeta_2^2)}$, $\Delta_1 = \zeta_1^2 + (\zeta_2 - \alpha)^2$, $\Delta_2 = \zeta_1^2 + (\zeta_2 + \alpha)^2$, $\Delta_3 = \alpha(2\zeta_1^2 + \alpha\zeta_2) - \zeta_2(\zeta_1^2 + \zeta_2^2)$, $\Delta_4 = \zeta_2(\zeta_1^2 + \zeta_2^2) - 2(2\zeta_1^2 + \zeta_2^2)\alpha + \zeta_2\alpha^2$, $\Delta_5 = (\zeta_2^2 - \zeta_1^2)(\zeta_1^2 + \zeta_2^2 - \alpha^2) - 4\alpha\zeta_2\zeta_1^2$, $\Delta_6 = 3\zeta_2(\zeta_1^2 + \zeta_2^2) - 2\alpha(\zeta_1^2 + 2\zeta_2^2) + \zeta_2\alpha^2$, $\Delta_7 = -(\zeta_1^2 + \zeta_2^2)(\zeta_1^2 - 5\zeta_2^2) - 4\zeta_2(\zeta_1^2 + 2\zeta_2^2)\alpha + (\zeta_1^2 + 3\zeta_2^2)\alpha^2$, $\Delta_8 = 3\zeta_2(\zeta_1^2 + \zeta_2^2) - 2(2\zeta_1^2 + 3\zeta_2^2)\alpha + 3\zeta_2\alpha^2$ and $\Delta_9 = (\zeta_1^2 + \zeta_2^2)(\zeta_1^2 + 4\zeta_2^2) - 2\zeta_2(3\zeta_1^2 + 4\zeta_2^2)\alpha + (\zeta_1^2 + 4\zeta_2^2)\alpha^2$.

[1] C. Kharif, E. Pelinovsky, and A. Slunyaev, *Rogue Waves in the Ocean* (Springer, Heidelberg, 2009).

[2] M. Onorato, S. Residori, U. Bortolozzo, A. Montina, and F. T. Arecchi, Rogue waves and their generating mechanisms in different physical contexts, Phys. Rep. **528**, 47 (2013).

[3] A. Chabchoub, N. P. Hoffmann, and N. Akhmediev, Rogue Wave Observation in a Water Wave Tank, Phys. Rev. Lett. **106**, 204502 (2011).

[4] Y. V. Bludov, V. V. Konotop, and N. Akhmediev, Matter rogue waves, Phys. Rev. A **80**, 033610 (2009).

[5] H. Bailung, S. K. Sharma, and Y. Nakamura, Observation of Peregrine Solitons in a Multicomponent Plasma with Negative Ions, Phys. Rev. Lett. **107**, 255005 (2011).

[6] D. R. Solli, C. Ropers, P. Koonath, and B. Jalali, Optical rogue waves, Nature **450**, 1054 (2007).

[7] B. Kibler, J. Fatome, C. Finot, G. Millot, F. Dias, G. Genty, N. Akhmediev, and J. M. Dudley, The Peregrine soliton in nonlinear fibre optics, Nat. Phys. **6**, 790 (2010).

[8] D. H. Peregrine, Water waves, nonlinear Schrödinger equations and their solutions, J. Aust. Math. Soc. B **25**, 16 (1983).

[9] N. Akhmediev, B. Kibler, F. Baronio, M. Belić, W.-P. Zhong, Y. Zhang, W. Chang, J. M. Soto-Crespo, P. Vouzas, P. Grelu *et al.*, Roadmap on optical rogue waves and extreme events, J. Opt. **18**, 063001 (2016).

[10] S. Chen, F. Baronio, J. M. Soto-Crespo, P. Grelu, and D. Mihalache, Versatile rogue waves in scalar, vector, and multi-dimensional nonlinear systems, J. Phys. A: Math. Theor. **50**, 463001 (2017).

[11] A. Chabchoub and N. Akhmediev, Observation of rogue wave triplets in water waves, Phys. Lett. A **377**, 2590 (2013).

[12] A. Chabchoub, N. Hoffmann, M. Onorato, A. Slunyaev, A. Sergeeva, E. Pelinovsky, and N. Akhmediev, Observation of a hierarchy of up to fifth-order rogue waves in a water tank, Phys. Rev. E **86**, 056601 (2012).

[13] N. Akhmediev, A. Ankiewicz, and J. M. Soto-Crespo, Rogue waves and rational solutions of the nonlinear Schrödinger equation, Phys. Rev. E **80**, 026601 (2009).

[14] D. J. Kedziora, A. Ankiewicz, and N. Akhmediev, Second-order nonlinear Schrödinger equation breather solutions in the degenerate and rogue wave limits, Phys. Rev. E **85**, 066601 (2012).

[15] P. Dubard, P. Gaillard, C. Klein, and V. B. Matveev, On multi-rogue wave solutions of the NLS equation and positon solutions of the KdV equation, Eur. Phys. J. Spec. Top. **185**, 247 (2010).

[16] B. L. Guo, L. M. Ling, and Q. P. Liu, Nonlinear Schrödinger equation: Generalized Darboux transformation and rogue wave solutions, Phys. Rev. E **85**, 026607 (2012).

[17] Y. Ohta and J. K. Yang, General high-order rogue waves and their dynamics in the nonlinear Schrödinger equation, Proc. R. Soc. Lond. A **468**, 1716 (2012).

[18] J. S. He, H. R. Zhang, L. H. Wang, K. Porsezian, and A. S. Fokas, Generating mechanism for higher-order rogue waves, Phys. Rev. E **87**, 052914 (2013).

[19] B. L. Guo and L. M. Ling, Rogue wave, breathers and bright-dark-rogue solutions for the coupled Schrödinger equations, Chin. Phys. Lett. **28**, 110202 (2011).

[20] L. M. Ling, B. L. Guo, and L. C. Zhao, High-order rogue waves in vector nonlinear Schrödinger equations, Phys. Rev. E **89**, 041201 (2014).

[21] F. Baronio, A. Degasperis, M. Conforti, and S. Wabnitz, Solutions of the Vector Nonlinear Schrödinger Equations: Evidence for Deterministic Rogue Waves, Phys. Rev. Lett. **109**, 044102 (2012).

[22] L. C. Zhao and J. Liu, Rogue-wave solutions of a three-component coupled nonlinear Schrödinger equation, Phys. Rev. E **87**, 013201 (2013).

[23] L. C. Zhao, B. L. Guo, and L. M. Ling, High-order rogue wave solutions for the coupled nonlinear Schrödinger equations-II, J. Math. Phys. **57**, 043508 (2016).

[24] L. M. Ling, L. C. Zhao, and B. L. Guo, Darboux transformation and classification of solution for mixed coupled nonlinear Schrödinger equations, Commun. Nonlin. Sci. Numer. Simulat. **32**, 285 (2016).

[25] G. Mu, Z. Y. Qin, and R. Grimshaw, Dynamics of rogue waves on a multisoliton background in a vector nonlinear Schrödinger equation, SIAM J. Appl. Math. **75**, 1 (2015).

[26] F. Baronio, M. Conforti, A. Degasperis, and S. Lombardo, Rogue Waves Emerging from the Resonant Interaction of Three Waves, Phys. Rev. Lett. **111**, 114101 (2013).

[27] A. Degasperis and S. Lombardo, Rational solitons of wave resonant-interaction models, Phys. Rev. E **88**, 052914 (2013).

[28] S. Chen, Y. Ye, F. Baronio, Y. Liu, X. M. Cai, and P. Grelu, Optical Peregrine rogue waves of self-induced transparency in a resonant erbium-doped fiber, Opt. Express **25**, 29687 (2017).

[29] S. Chen, P. Grelu, and J. M. Soto-Crespo, Dark-and bright-rogue-wave solutions for media with long-wave-short-wave resonance, Phys. Rev. E **89**, 011201 (2014).

[30] K. W. Chow, H. N. Chan, D. J. Kedziora, and R. H. J. Grimshaw, Rogue wave modes for the long wave-short wave resonance model, J. Phys. Soc. Jpn. **82**, 074001 (2013).

[31] J. C. Chen, Y. Chen, B. F. Feng, and K. Maruno, General high-order rogue wave of the (1+1)-dimensional Yajima-Oikawa system, J. Phys. Soc. Jpn. **87**, 094007 (2018).

[32] X. Wang, Y. Q. Li, F. Huang, and Y. Chen, Rogue wave solutions of AB system, Commun. Nonlin. Sci. Numer. Simulat. **20**, 434 (2015).

[33] X. Y. Wen and Z. Y. Yan, Modulational instability and higher-order rogue waves with parameters modulation in a coupled integrable AB system via the generalized Darboux transformation, Chaos **25**, 123115 (2015).

[34] F. Baronio, Akhmediev breathers and Peregrine solitary waves in a quadratic medium, Opt. Lett. **42**, 1756 (2017).

[35] B. Frisquet, B. Kibler, P. Morin, F. Baronio, M. Conforti, G. Millot, and S. Wabnitz, Optical dark rogue waves, Sci. Rep. **6**, 20785 (2016).

[36] F. Baronio, B. Frisquet, S. Chen, G. Millot, S. Wabnitz, and B. Kibler, Observation of a group of dark rogue waves in a telecommunication optical fiber, Phys. Rev. A **97**, 013852 (2018).

[37] V. E. Zakharov and L. A. Ostrovsky, Modulation instability: The beginning, Physica D **238**, 540 (2009).

[38] F. Baronio, M. Conforti, A. Degasperis, S. Lombardo, M. Onorato, and S. Wabnitz, Vector Rogue Waves and Baseband Modulation Instability in the Defocusing Regime, Phys. Rev. Lett. **113**, 034101 (2014).

[39] F. Baronio, S. Chen, P. Grelu, S. Wabnitz, and M. Conforti, Baseband modulation instability as the origin of rogue waves, Phys. Rev. A **91**, 033804 (2015).

[40] L. C. Zhao and L. Ling, Quantitative relations between modulational instability and several well-known nonlinear excitations, J. Opt. Soc. Am. B **33**, 850 (2016).

[41] G. Biondini and D. Mantzavinos, Universal Nature of the Nonlinear Stage of Modulational Instability, Phys. Rev. Lett. **116**, 043902 (2016).

[42] B. Frisquet, B. Kibler, J. Fatome, P. Morin, F. Baronio, M. Conforti, G. Millot, and S. Wabnitz, Polarization modulation instability in a Manakov fiber system, Phys. Rev. A **92**, 053854 (2015).

[43] D. J. Benney, Significant interactions between small and large scale surface saves, Stud. Appl. Math. **55**, 93 (1976).

[44] D. J. Benney, A general theory for interactions between short and long waves, Stud. Appl. Math. **56**, 81 (1977).

[45] N. Yajima and M. Oikawa, Formation and interaction of Sonic-Langmuir solitons: Inverse scattering method, Prog. Theor. Phys. **56**, 1719 (1976).

[46] A. C. Newell, Long waves-short waves: A solvable model, SIAM J. Appl. Math. **35**, 650 (1978).

[47] A. C. Newell, The general structure of integrable evolution equations, Proc. R. Soc. Lond. A **365**, 283 (1979).

[48] J. C. Chen, B. F. Feng, K. Maruno, and Y. Ohta, The derivative Yajima-Oikawa dystem: Bright, dark soliton and breather solutions, Stud. Appl. Math. **141**, 145 (2018).

[49] X. Huang, B. L. Guo, and L. M. Ling, Darboux transformation and novel solutions for the long wave-short wave model, J. Nonlin. Math. Phys. **20**, 514 (2013).

[50] A. R. Chowdhury and P. K. Chanda, To the complete integrability of long-wave-short-wave interaction equations, J. Math. Phys. **27**, 707 (1986).

[51] L. M. Ling and Q. P. Liu, A long waves-short waves model: Darboux transformation and soliton solutions, J. Math. Phys. **52**, 053513 (2011).

[52] J. Y. Zhu and Y. G. Kuang, Cusp solitons to the long-short waves equation and the ∂-dressing method, Rep. Math. Phys. **75**, 199 (2015).

[53] X. G. Geng and H. Wang, Algebro-geometric constructions of quasi-periodic flows of the Newell hierarchy and applications, IMA J. Appl. Math. **82**, 97 (2017).